



The Lewis number under supercritical conditions

K. Harstad, J. Bellan*

Jet Propulsion Laboratory, California Institute of Technology, Pasadena, CA 91109, U.S.A.

Received 20 January 1998; in final form 13 July 1998

Abstract

An effective Lewis number is calculated for situations where temperature and mass fraction gradients are very large by defining effective thermal and mass diffusivities; such situations may occur in systems where there is more than one chemical component, and in particular under supercritical conditions. The definitions evolve from a model assuming that derivatives of certain functions are small with respect to those of the dependent variables. In the model, Soret and Dufour effects are included and Shvab–Zeldovich-like variables are defined to remove the coupling between the operators of the differential equations for temperature and mass fractions. Results from calculations using binary systems of chemical components, using both isolated fluid drops and interacting fluid drops, show that under supercritical conditions, depending upon the compounds, the effective Lewis number can be 2–40 times larger than the traditionally calculated Lewis number and that the spatial variation of the two numbers is different. For the values of the thermal diffusion factor used in the calculations, the Soret and Dufour effects are negligible; the discrepancy between the traditional and effective Lewis numbers is due to the combined effect of the small mass diffusion factor and the difference between the specific enthalpies of the two compounds. Parametric variations show that the effective Lewis number increases with increasing pressure and decreasing surrounding gas temperature. Closer drop proximity in clusters results in sharper peaks in the effective Lewis number due to the increased gradients of the dependent variables. © 1998 Elsevier Science Ltd. All rights reserved.

Nomenclature

C_p molar heat capacity at constant pressure
 D diffusion coefficient
 F_{ems} emission flux
 h molar enthalpy
 J molar flux
 L elements of the transport matrix
 Le Lewis number
 m molar mass
 Ma Mach number
 n number of moles per unit volume
 N number of species
 Nu_C Nusselt number
 p pressure
 q heat flux
 r generic coordinate
 R_d fluid entity radius

R_u universal gas constant
 t time
 T temperature
 u velocity
 v molar volume
 X mole fraction
 Y mass fraction.

Greek symbols

α_D mass diffusion factors
 α_T thermal diffusion factor
 α_v thermal expansion ratio
 β $1/(R_u/T)$
 γ activity coefficient
 Δr grid size
 η viscosity
 λ thermal conductivity
 μ chemical potential
 ρ density
 τ stress tensor
 Φ_v viscous dissipation.

* Corresponding author. Tel.: 001 818 354 6959; fax: 001 818 393 5011; e-mail: josette.bellan@jpl.nasa.gov

Subscripts

- b fluid entity interface, at $r = R_d$
- c critical point property
- C cluster
- d fluid drop
- e external
- eff effective
- i, j species
- m mass
- si at the edge of the sphere of influence
- T thermal.

Superscripts

- i, j species
- 0 initial value
- + (–) on the pure $\text{LO}_x(\text{H}_2)$ side of $r = R_d$.

1. Introduction

The Lewis number is a measure of the importance of heat diffusion to the mass diffusion, $Le \equiv D_T/D_m$ where traditionally $D_T = \lambda/(nC_p)$; therefore Le provides an indication of what process controls a phenomenon being studied. For example, in gases usually $Le = O(1)$ which means that heat and mass diffusion proceed at similar rates. Departures from unity Le in gases have been discussed by Law et al. [1], Haworth and Poinso [2], Lee et al. [3], Joulin [4], Echekki and Freziger [5] and others in the context of curved flames; and by Greenberg and Ronney [6] in the context of flame spread over thin and thick solid fuels. In contrast to gases, in liquids $Le = O(10)$ – $O(100)$ indicating that heat diffusion is faster than mass diffusion.

All existing studies of Le effects in gases have discussed departures from the preferred unity assumption (because it enables an easier mathematical treatment), but none has questioned the validity of the Le calculation according to the above relationships for portraying the relative importance of heat and mass diffusion. This is because the calculation of the Lewis number for gases and liquids is straightforward when the molar flux depends only upon the mole fraction gradients and the heat flux depends only upon the temperature gradient. However, this is not the most general situation, and is certainly not applicable to a general fluid. The present study is devoted to the investigation of departures from the traditional calculation of Le ; we address here the case of general fluids. Because liquids and gases at atmospheric conditions become fluids at supercritical conditions, this study is in particular relevant to multicomponent systems at very high pressures and temperatures characteristic of supercritical conditions. We are particularly interested in the behavior of compounds under supercritical conditions because of the relevance to liquid rocket propulsion, gas turbine engines and diesel engines.

Fluctuation–dissipation theory provides the most general framework for defining the heat and mass diffusion coefficients. The viewpoint of fluctuation theory is intermediate to that of continuum and molecular-level approaches and allows the modeling of transport processes totally consistent with nonequilibrium thermodynamics (which continuum theory does not address); at the same time it avoids the difficulties (and some of the potential benefits, which are irrelevant here) of molecular dynamics. For example: continuum theory does not give relationships between fluxes and forces for a general fluid; it is customary within the continuum formulation to extend kinetic theory of rarified gases to describe more general cases (as in [7]). Within the formalism of Keizer's fluctuation–dissipation theory [8, 9], the mass diffusivity and thermal diffusivity appear in elements of a transport matrix that relates the gradients of the chemical potentials and of the temperature to the molar and heat fluxes as follows:

$$\mathbf{J}_i = L_{iq} \nabla \beta - \sum_{j=1}^N L_{ij} \nabla (\beta \mu_j), \quad \mathbf{q} = L_{qq} \nabla \beta - \sum_{j=1}^N L_{qj} \nabla (\beta \mu_j) \quad (1.1)$$

where L_{ij} are the Fick's diffusion elements, L_{qq} is the Fourier thermal diffusion element, L_{iq} are the Soret diffusion and L_{qj} are the Dufour diffusion elements. The Onsager relations state that $L_{ij} = L_{ji}$ and $L_{iq} = L_{qi}$. From conservation of total and species mass in the system one obtains the additional relations $\sum_i^N m_i \mathbf{J}_i = \mathbf{0}$ and $\sum_i^N L_{ij} m_i = 0$ for $j \in [1, N]$ and $j = q$.

Using the thermodynamic relationship

$$d(\beta \mu_j) = \beta (v_j dp - h_j d \ln T) + \left(\sum_{i=1}^{N-1} \alpha_{D_i} dX_i \right) / X_j \quad (1.2)$$

where

$$\alpha_{D_i} \equiv \beta X_i \partial \mu_i / \partial X_j = \partial X_i / \partial X_j + X_i \partial \ln \gamma_i / \partial X_j \quad (1.3)$$

one can calculate \mathbf{J}_i from (1.1) and (1.2). Equations (1.1)–(1.3) show another benefit of fluctuation theory in that the relationship between fluxes and thermodynamics is obvious; basically, the theory consistently extends gradient transport to far from equilibrium situations. Within this framework, the expressions for the chemical potentials can be derived for a general fluid and used in equation (1.2), which allows the consideration of both possibly non-unity diffusion factors and transport effects of the enthalpy and molar volumes with temperature gradients and pressure gradients, respectively.

This formalism shows that the classical calculation of Le can no longer indicate the relative importance of heat and mass diffusion because of the additional contributions that appear as non-diagonal terms. Thus, there is a need to identify what is the equivalent of D_T and D_m under general conditions, and investigate characteristic values of their ratio, called here Le_{eff} .

In this paper we present a formalism for a calculation of Le_{eff} and show that under supercritical conditions the existence of the nondiagonal terms in the transport equations enhances the heat diffusion and decreases the mass diffusion, resulting in Le_{eff} larger than Le by a factor that varies from approximately 2–40 depending on the compounds and on the particular conditions of the calculation. Additionally, we show that Le_{eff} is a non-monotonic function of Le , and thus that the variation of Le cannot be considered to represent even a relative qualitative estimate of the importance of heat and mass diffusion. In Section 2 we develop the expression for Le_{eff} for a binary component fluid in a general one-dimensional geometry; the analysis can be easily extended to a multicomponent fluid in multidimensions. In Section 3 we calculate Le_{eff} for both isolated and collections of spherical entities (fluid drops) of LO_x in fluid H_2 at high pressures and investigate the importance of the thermal diffusion factor upon the results. Results are also presented for isolated C_7H_{16} fluid drops in fluid N_2 to identify the impact of the compounds identity upon the results. Finally, Section 4 is devoted to conclusions.

2. Model

In a single coordinate configuration, the species and energy equations for a binary component fluid can be written as follows:

$$\rho \frac{\partial Y_1}{\partial t} + \rho u \frac{\partial Y_1}{\partial r} = m_1 \nabla \cdot \mathbf{J}, \quad \rho \frac{\partial Y_2}{\partial t} + \rho u \frac{\partial Y_2}{\partial r} = -m_1 \nabla \cdot \mathbf{J} \quad (2.1)$$

$$n C_p \left(\frac{\partial T}{\partial t} + u \frac{\partial T}{\partial r} \right) = \alpha_v T \left(\frac{\partial p}{\partial t} + u \frac{\partial p}{\partial r} \right) - \nabla \cdot \mathbf{q} + \Phi_v - m_1 (h_1/m_1 - h_2/m_2) \nabla \cdot \mathbf{J} \quad (2.2)$$

where $\alpha_v = [(\partial v / \partial T)_{p,x_i}] / v$, $J = -J_{1r} = (m_2/m_1) J_{2r}$. As shown by equation (1.1), the general forms of J and $q = -q_r$ are

$$J = A_J \frac{\partial Y_1}{\partial r} + B_J \frac{\partial T}{\partial r} + C_J \frac{\partial p'}{\partial r}$$

$$q = A_q \frac{\partial T}{\partial r} + C_q \frac{\partial Y_1}{\partial r} + B_q \frac{\partial p'}{\partial r}. \quad (2.3)$$

Expressions of the gradients multiplicative coefficients in equation (2.3) appear in the Appendix.

The terms proportional to the gradients of the dynamic pressure in the expressions for J and q will be neglected in the following because those gradients are proportional to Ma^2 and $Ma \ll 1$, while coefficients C_J and B_q are no larger than other coefficients in the equations; spatial variations of p' were confirmed to be small by results from calculations of isolated entities of LO_x in fluid H_2 at high pressures [10]. The viscous dissipation term has

been neglected as well because it is expected to be much smaller than the other terms in equation (2.2).

If the set $\Gamma = (Y_1, T)$ is considered a vector primitive variable, the differential operator $\mathcal{L}\Gamma = \rho \partial \Gamma / \partial t + \rho u \partial \Gamma / \partial r - (1/r^s) \partial (r^s \mathcal{D} \partial \Gamma / \partial r) / \partial r$, where $s = 0$ for planar geometry and $s = 2$ for spherical geometry, represents the set of conservation equations $\mathcal{L}\Gamma = 0$, where \mathcal{D} is a generic diffusion coefficient matrix. When Fick's and Fourier's laws accurately describe molar and heat fluxes, respectively, the operators for the two variables Y_1 and T are uncoupled because the diffusion term in the equation for each variable contains only derivatives of that variable; \mathcal{D} is diagonal. In that situation, one defines the traditional Le as the ratio of the diffusive length scales of the temperature and mass fractions; the ratio is calculated using the coefficients of the diffusive terms. In the more general situation where the flux matrix is given by equation (2.3) instead of the Fick and Fourier laws, the differential operators for the two variables are no longer uncoupled because in each equation the diffusion term contains derivatives of both variables. The differential operators are now coupled, and this coupling prohibits a simple definition of appropriate diffusion length scales for heat and mass transfer.

Similar to the classical situation where Le relates the diffusive length scales of the mass fractions and temperature given by the coefficients of the diffusive terms when the differential operators of the species and temperature equations are uncoupled, and thus the diffusion term in the differential operator is given by multiplying a diagonal matrix with the spatial derivative, one must find here equivalent variables for which the matrix of the system of equations (2.1) and (2.2) has a diagonal form. Given the complexity of equations (2.1)–(2.3), a simple, accurate combination of variables cannot be found a priori. Tambour and Gal-Or [11] have performed such a diagonalization for compressible, laminar boundary layers and stagnation flows with blowing or suction; the same method was used by Greenberg et al. [12] in laminar jets and by Greenberg [13] for planar premixed gaseous flames. Similar to the previous work [11–13], the strategy is here to find a solution that will be valid under certain assumptions.

The first assumption is that of a boundary layer spatial variation at a location that would be a surface under subcritical conditions, $r = R_d$, in which case the medium for $r < R_d$ is a liquid (component 1) and the medium for $r > R_d$ is a gas (component 2). The analysis will then be valid for $|R_d - r| \ll R_d$. In subcritical conditions, the liquid evaporates (except for the particular case of saturation) and thus $\rho u = F_{\text{ems}}$; under supercritical conditions for component 1, one may still define the flux in the same manner although its meaning is not necessarily that of evaporation (depending on the surface mixture critical point). The second assumption is that of quasi-steady behavior; although under supercritical conditions a

quasi-steady behavior is not necessarily attained (because the value of the density ratio $\rho(R_d^+)/\rho(R_d^-)$ does not remain $\ll 1$ during the calculation), this assumption is appropriate for finding order of magnitude scales rather than an entirely accurate solution for the variables. It is the form of the steady, convection–diffusion equation solution that provides the intuition about the assumptions to be further made in the model. This form is an exponential dependence on a spatial integral multiplied by a more weakly varying function [15].

The point of departure for finding an approximate solution are Shvab–Zeldovich-like variables [7] that are combinations of Y_1 and T . In the Shvab–Zeldovich formalism for transient combustion in a diffusive–convective system, linear combinations of variables are used in conjunction with a series of assumptions to eliminate the reaction term from all but one equation and render the conservation equations easier to solve. In the present context, the combined variables

$$\Omega_Y \equiv Y_1 - \omega_T T \quad \text{and} \quad \Omega_T \equiv T - \omega_Y Y_1 \quad (2.4)$$

are defined to diagonalize the operators of the differential equations; the quantities ω_T and ω_Y are calculated below by satisfying the conservation equations. Once equations (2.4) are replaced into the original equations (2.1)–(2.3), Ω_Y and Ω_T can be shown to be approximately governed by the following equations for appropriately chosen ω_T and ω_Y

$$\rho \frac{\partial \Omega_Y}{\partial t} + F_{\text{ems}} \frac{\partial \Omega_Y}{\partial r} = \frac{1}{r^s} \frac{\partial}{\partial r} \left(r^s \rho D_{\text{eff}} \frac{\partial \Omega_Y}{\partial r} \right) \quad (2.5)$$

$$\rho \frac{\partial \Omega_T}{\partial t} + F_{\text{ems}} \frac{\partial \Omega_T}{\partial r} = \frac{1}{r^s} \frac{\partial}{\partial r} \left[r^s (m \lambda_{\text{eff}}/C_p) \frac{\partial \Omega_T}{\partial r} \right]. \quad (2.6)$$

Equations (2.5) and (2.6) are obtained under the assumption that spatial and temporal derivatives of functions ω_T and ω_Y are smaller than those of Ω_Y and Ω_T and can thus be neglected. This assumption is satisfied if equations (2.5) and (2.6) are quasi-steady and if the multipliers of the exponential functions which are the characteristic solutions of the diffusion–convection equation have a smaller variation than the exponential functions. Quasi-steadiness of equations (2.5) and (2.6) is satisfied if $(F_{\text{ems}})^2 \gg \rho^2 D_{\text{eff}} \partial/\partial t$ and $(F_{\text{ems}})^2 \gg (m \rho \lambda_{\text{eff}}/C_p) \partial/\partial t$. Small variation of the multipliers with respect to the exponential functions occurs if $F_{\text{ems}} \Delta r > \rho D_{\text{eff}}$ and $F_{\text{ems}} \Delta r > m \lambda_{\text{eff}}/C_p$, where Δr is the grid size.

The effective transport coefficients in equations (2.5) and (2.6) are calculated from the original equations as follows:

$$\rho D_{\text{eff}} = m_1 A_J - \omega_T m C'_q/C_p \quad (2.7)$$

$$\lambda_{\text{eff}} = A'_q - \omega_Y (m_1/m) C_p B_J \quad (2.8)$$

where

$$A'_q \equiv A_q - m_1 (h_1/m_1 - h_2/m_2) B_J \quad (2.9)$$

and

$$C'_q \equiv C_q - m_1 (h_1/m_1 - h_2/m_2) A_J$$

with

$$\omega_T = \sigma m_1 C_p B_J/m \quad \text{and} \quad \omega_Y = -\sigma C'_q \quad (2.10)$$

where σ is the positive root of the second-order algebraic equation

$$(m_1/m) C_p B_J C'_q \sigma^2 + [A'_q - (m_1/m) C_p A_J] \sigma - 1 = 0 \quad (2.11)$$

the other root being unphysical as it leads to singular behavior. These equations allow the calculation of D_{eff} , λ_{eff} and $Le_{\text{eff}} \equiv \lambda_{\text{eff}}/(n C_p D_{\text{eff}})$ once the values of the dependent variables are known.

Although the above analysis is strictly valid only within a boundary layer, it is also conceptually correct in any region where there are large variations of the dependent variables. Thus, the above expressions show the correct transport scales for any region of steep gradients. As such, the ratio of the effective transport coefficients will be calculated below and compared to that of the conventional transport coefficients for specific situations involving large dependent variable gradients.

To illustrate the model, calculations are performed for spherical fluid drops, either isolated or in clusters where they may collectively interact. The general model for isolated fluid drops is described in [10] and is based upon the fluctuation–dissipation theory discussed above whose main results are equations (2.1)–(2.3). Additional to the conservation equations (2.1) and (2.2), the model of Harstad and Bellan [10] also solves a mass conservation equation. The boundary conditions at the evolving interface initially between pure LO_x and mainly H_2 fluid, and in the far field are also described in detail in [10]. The calculation of the equations of state is described elsewhere [17] and the models for the transport coefficients is discussed in Harstad and Bellan [10]. For cluster studies, there are additional mass, species and energy conservation equations relating the behavior of all entities in the cluster [14], the boundary conditions between the cluster and its surrounds.

3. Results

To illustrate the difference between the traditional Le and Le_{eff} we present calculations obtained from the solution of isolated fluid drops and clusters of fluid drops of LO_x in H_2 at supercritical conditions. In order to evaluate the importance of the Soret and Dufour terms, we also present results from isolated fluid drop calculations with null α_T as well as with one non null value smaller than the baseline choice of $\alpha_T = 0.05$ [16]. Finally, to investigate possible departures from the conclusions based on results from the LO_x – H_2 system, we also present results for isolated C_7H_{16} fluid drops in fluid N_2 ; obviously, a myriad of binary systems can be investigated and by its nature the present study cannot be exhaustive.

3.1. Isolated fluid drops: the LO_x-H_2 system

3.1.1. Baseline behavior

Figure 1 illustrates the radial variation of Le and Le_{eff} at different times for an isolated fluid drop having $R_d^0 = 50 \times 10^{-4}$ cm and $T_{d,b}^0 = 100$ K (the fluid drop temperature is assumed initially uniform), in far field surroundings characterized by $T_{si}^0 = 1000$ K, $p = 80$ MPa and $Y_{si}^0 = 0$. The fluid drop is initially composed of pure LO_x ($T_c = 154.6$ K, $p_c = 5.043$ MPa), while the surrounding is hydrogen ($T_c = 33.2$ K, $p_c = 1.313$ MPa); in

order to avoid an initial unphysical discontinuity, a small amount of oxygen exists initially in the drop surroundings, its distribution vanishing with increasing r . The far field conditions $T_c = 1000$ K and $Y_{1c} = 0$ are at a distance $(R_{si}^0 - R_d^0)$ from the drop interface, where $R_{si}^0 = 0.1$ cm.

The spatial variation of Le_{eff} is essentially different from that of Le in that it is nonmonotonic even after the memory of the initial condition is lost [the $t = 0$ curves do not appear in any of the Le_{eff} plots, throughout this study, because the value of $Le_{eff}(r = R_d^0)$ is off scale]. This is because Le_{eff} implicitly accounts for Y_1 and T gradient effects; these Y_1 and T gradients do not occur at the same location under supercritical conditions. Thus, the spatial variation of Le_{eff} is directly related to the variation of Y_1 and T gradients as follows: for small r , the shallow part of the curves corresponds mostly to the large $\partial T/\partial r$, Y_1 being mostly uniform, the temporal increase of Le_{eff} is due to the increased T . The strongly increasing branch of Le_{eff} corresponds to the region of large $\partial Y_1/\partial r$ and the location of the maximum Le_{eff} is directly related to the maximum Y_1 gradient. Finally, the decreasing part of the Le_{eff} curves corresponds to the decreasing $\partial Y_1/\partial r$ and the asymptotic leveling of T . In contrast, the Le spatial variation reflects only the dependence of D_T and D_m upon composition and T . An elimination of the spatial variation between Le and Le_{eff} results in the plots presented in Fig. 1(c): Le_{eff} vs Le at different times. Examination of the curves in Fig. 1 indicates that the additional coupling terms result in an enhancement of the thermal diffusivity with respect to the mass diffusivity. More precisely, tedious manipulations of equations (2.7)–(2.11) and (A.1)–(A.6) in the Appendix show that in fact the thermal diffusivity is effectively increased whereas the mass diffusivity is effectively decreased. For the conditions used to obtain the results depicted in Fig. 1, the ratio Le_{eff}/Le is approximately 20 in the inner part of the interface, whereas on the outer side of the interface it reaches a maximum of 60 and a minimum of three.

The fact that Le is a multivalued function of Le_{eff} (see Fig. 1(c)) is a warning that Le cannot be even considered a qualitative estimate of the true relative importance of heat to mass diffusion at different spatial locations. Moreover, whereas the values of Le_{eff} indicate that heat diffusion exceeds mass diffusion at all locations, Le indicates erroneously that mass diffusion dominates heat diffusion at all times for $r \leq R_d^0$. The almost-complete coincidence of all curves in Fig. 1(c) indicates that for a given geometry and initial conditions, at each spatial position there is an almost-unique relationship between the ratio of the transport coefficients and the ratio of the effective transport coefficients (but not vice versa). Since both the transport coefficients and the effective transport coefficients depend upon Y_1 and T (whose variation is governed by the conservation equations) this coincidence is not obvious and its meaning is not immediately appar-

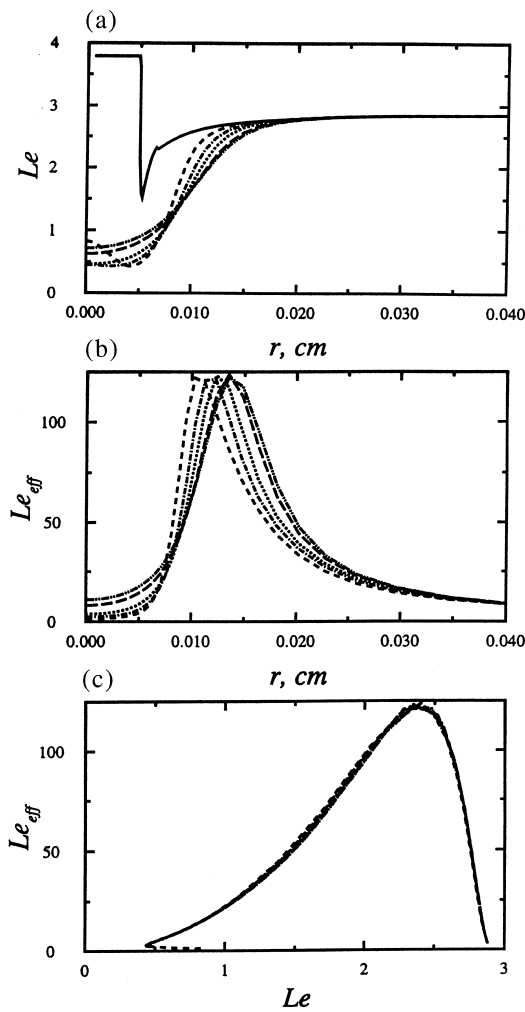


Fig. 1. Spatial variation of the traditional (a) and the effective (b) Lewis numbers, and the variation of Le_{eff} with Le (c) at various times for $R_d^0 = 50 \times 10^{-4}$ cm, $R_{si}^0 = 0.1$ cm, $T_{d,b}^0 = 100$ K, $T_{si}^0 = 1000$ K, $Y_{si}^0 = 0$, and $p = 80$ MPa. The curves correspond to the following times: 0.0 s (—), 6×10^{-3} s (---), 1.0×10^{-2} s (-·-·-), 1.4×10^{-2} s (· · ·), 2.0×10^{-2} s (— · —), 2.31×10^{-2} s (-·-·-).

ent. Further results presented below for the $C_7H_{16}-N_2$ system indicate that this self-similarity is not a property of the conservation equations and is instead related to the system of compounds.

3.1.2. Parametric variation

Plots of Le and Le_{eff} at $t = 2 \times 10^{-2}$ s for same initial conditions as the baseline calculations except for p , appear in Fig. 2. Increasing p decreases both D_m and D_T

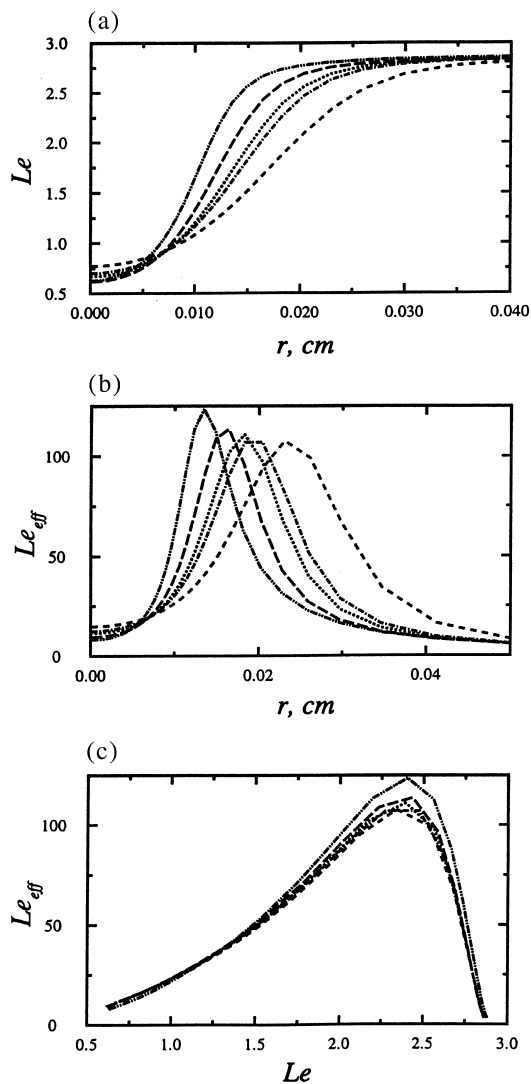


Fig. 2. Spatial variation at 2×10^{-2} s of the traditional (a) and the effective (b) Lewis numbers and the variation of the effective Lewis number with the traditional Lewis number (c) for several pressures: 10 MPa (---), 20 MPa (- · - · -), 25 MPa (- · -), 40 MPa (- - -), 80 MPa (- · · -). Other initial conditions are those in Fig. 1 caption.

(see Fig. 3), however, $D_T \equiv \lambda/(nC_p)$ is a stronger function of p . The spatial variation of all transport properties results from the different p in the far field, and from the combined effect of the different p upon the composition, ρ and T in the near field of the initial drop boundary [10]. In the inner region of mild gradients, both Le and Le_{eff} show similar variations, however, the absolute values differ by a factor of approximately 20. In the far field region (which similarly to the inner region has small gradients), both Le and Le_{eff} show an asymptotic behavior, their values differing by a factor of approximately three. The large difference of variation (approximately a factor of 50) occurs in the region of strong gradients in accord with the boundary layer analysis. The narrowing of the width between the increasing and the decreasing branches of Le_{eff} indicates the reduction in scales with increasing p . The variation of Le_{eff} with Le depicted in Fig. 2 indicates that in the low and high Le regime there is an almost unique relationship to Le_{eff} independent of p , whereas the influence of p is mainly felt in the intermediate Le regime which occurs in the region of large gradients.

Far field temperature effects upon the variation of Le and Le_{eff} are illustrated in Fig. 4 at $t = 2 \times 10^{-2}$ s for two

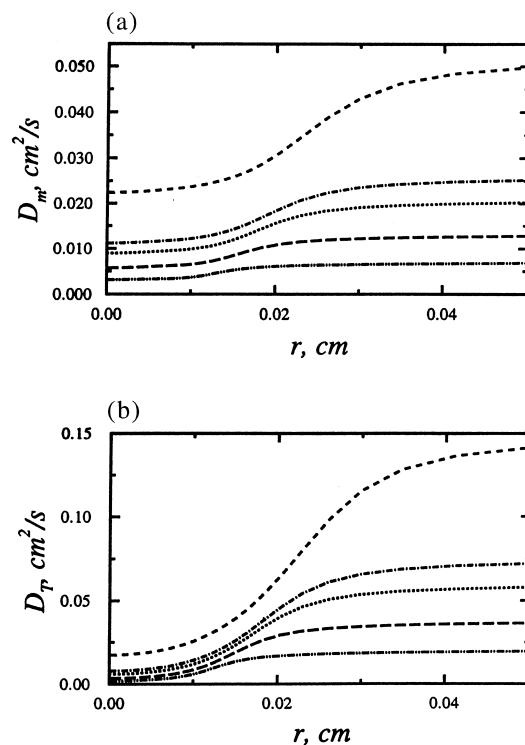


Fig. 3. Spatial variation of the mass (a) and thermal (b) diffusivities at 2×10^{-2} s for the conditions listed in the caption of Fig. 2; the curves are also labelled identically.

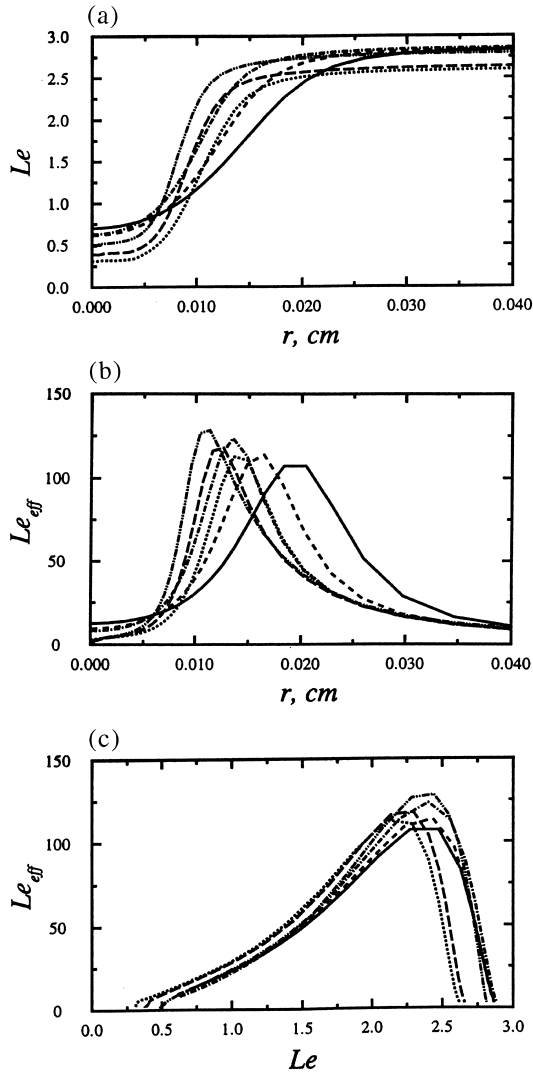


Fig. 4. Spatial variation at 2×10^{-2} s of the traditional (a) and the effective (b) Lewis numbers, and variation of the effective Lewis number with the traditional Lewis number (c) at 2×10^{-2} s. Plots are for two temperatures and three pressures; the other conditions are those listed in Fig. 1 caption. Curves are labelled as follows: $T_{si}^0 = 1000$ K (—), (---) and (-·-·-); and $T_{si}^0 = 500$ K (···), (- - -) and (-·-·-). Corresponding pressures are: 20 MPa (—) and (···); 40 MPa (---) and (- - -); and 80 MPa (-·-·-) and (-·-·-).

temperatures at three values of p . In the lower p range, the T and Y_1 gradients occur at increasing distance with increasing temperature, whereas in the higher p regime the distance between the largest gradients of T and Y_1 becomes less sensitive to temperature. Unlike the variation of Le_{eff} with Le as a function of p , the relationship between Le and Le_{eff} is sensitive to T_{si}^0 over the entire range of Le .

The variation of Le and Le_{eff} with the initial fluid drop size is depicted in Fig. 5 and shows the increase in scales with increasing initial size.

To investigate the importance of Soret and Dufour effects on the above results, calculations were performed with $\alpha_T = 0$ and 0.01 to compare with the baseline calculations where $\alpha_T = 0.05$. The results from the three sets of calculations were virtually indistinguishable indicating that for the range of α_T explored, the Soret and Dufour terms are negligible. This result is in apparent contradiction with the difference in magnitude and variation of Le and Le_{eff} . However, careful examination of equations (2.3) and (A.2) in the Appendix shows that the contribution to the molar flux from the temperature gradient contains two terms: the first is the difference in the ratios of the molar enthalpies divided by the molar masses, and the second is the Soret term. Spatial plots of the molar enthalpy (not presented) show that the LO_x molar enthalpy is smaller than that of H_2 . Since additionally the molar mass of oxygen is one order of magnitude larger than that of hydrogen, this renders the first term in equation (A.2) in the Appendix very large compared to the Soret term. Moreover, in equation (2.3) the multi-

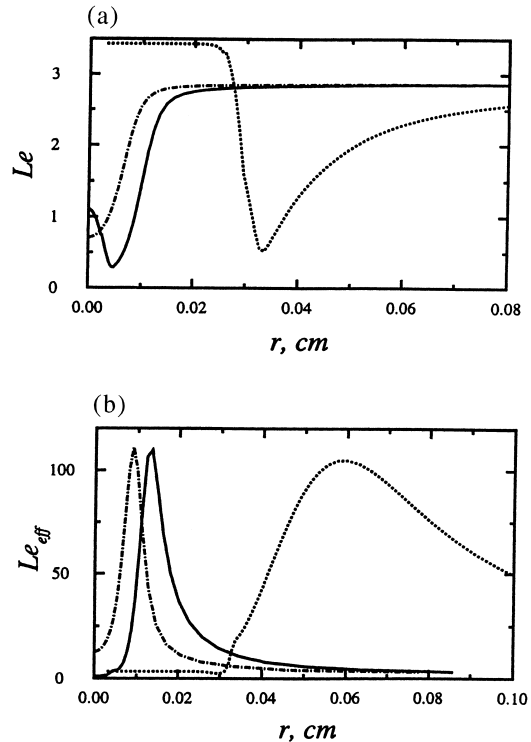


Fig. 5. Spatial variation at 2×10^{-2} s of the traditional (a) and the effective (b) Lewis numbers at 25 MPa for initial fluid drop radii 25×10^{-4} cm (-·-·-), 50×10^{-4} cm (—) and 300×10^{-4} cm (···). The other conditions are those of Fig. 1.

plicative coefficient of the mass fraction gradient, A_j , contains the factor α_D which is unity for a two component system under subcritical conditions [see equation (1.3)] but is $\ll 1$ under the present conditions; the small value of α_D also contributes to the large value of Le_{eff} [see equation (2.7)]. Such diffusion departures from the usual, subcritical behavior were discussed by Cussler [18] who points out that diffusion coefficients may approach a null value near and above the critical condition.

The present conclusions depend on the uncertain value range for α_T ; to our knowledge, there is no data providing α_T for the LO_x - H_2 system as a function of T , p and Y_1 .

3.2. Clusters of fluid drops: the LO_x - H_2 system

To investigate the effect of fluid drops proximity on the relative importance of both conventional and effective heat and mass diffusion, calculations were performed with spherical clusters of these drops. The details model for the fluid drops interactions is described elsewhere [14]; the only results discussed here are those pertinent to Le and Le_{eff} .

Due to the essentially diffusive behavior at supercritical conditions, interactions among fluid drops are not expected unless these are in close proximity. The proximity of the fluid drops is measured by a 'sphere of influence' around each drop that is centered at the drop center and has a radius, R_{si} , which is half of the distance between adjacent drops. Transfer from the cluster surroundings to the cluster is modeled using the Nusselt number concept [14]. As an example, in the baseline calculations with $R_d^0 = 50 \times 10^{-4}$ cm, $R_{\text{si}}^0 = 2R_d^0$, $R_C^0 = 2$ cm, $T_{\text{d,b}}^0 = 100$ K (T_d^0 is uniform inside the drop), $T_{\text{si}}^0 = T_c = 1000$ K, $p_c = 80$ MPa and $Y_{1c} = 0$, the number of drops in the cluster is 5.92×10^6 .

Results illustrating the difference in variation for both Le and Le_{eff} with increasing R_{si}^0/R_d^0 for two different pressures are depicted in Fig. 6. Decreasing R_{si}^0/R_d^0 results in an increase in Le and the effect is more pronounced at larger pressures, however the maximum value attained is always at the edge of the sphere of influence and remains constant with pressure and drop packing. In contrast, Le_{eff} attains its maximum inside the sphere of influence, at the location of maximum Y_1 gradients [14] as already explained above. Additionally, while the maximum Le_{eff} value remains constant with drop packing, it increases substantially with pressure in agreement with the known larger augmentation of heat diffusion with respect to mass diffusion as the pressure increases. Examination of Fig. 6(b) shows that a factor of four increase in pressure induces approximately a 25% increase in the maximum value of Le_{eff} .

Since gradients at the edge of the cluster boundary are influenced by Nu_C , the value of Nu_C was varied from 10^2 (baseline) to 10^5 in increments of factors of 10. The plots appearing in Fig. 7 show the relative insensitivity of the

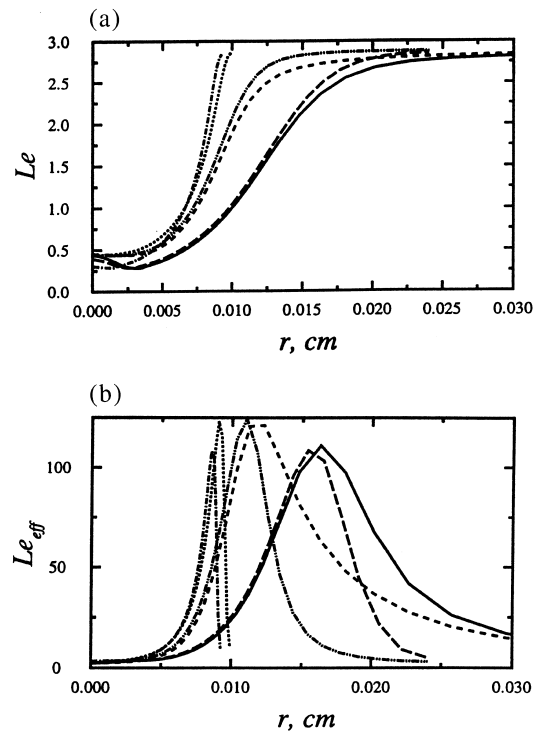


Fig. 6. Spatial variation at 10^{-2} s of the traditional (a) and the effective (b) Lewis numbers for clusters of drops having $R_d^0 = 50 \times 10^{-4}$ cm, $Nu_C = 10^2$, $R_C^0 = 2$ cm, $T_{\text{d,b}}^0 = 100$ K, $T_{\text{si}}^0 = T_c = 1000$ K and $Y_{\text{si}}^0 = Y_c = 0$. Curves are labelled as follows: $R_{\text{si}}^0/R_d^0 = 10$ (—) and (---); 5 (—) and (-·-·); 2 (-·-·) and (·-·). Two pressures are considered: 20 MPa (—), (---) and (-·-·); and 80 MPa (---), (-·-·) and (·-·).

results to Nu_C : it is only the size of the cluster that slightly increases (due to increased heat transfer, see [14]) when Nu_C changes by three orders of magnitude, but the maximum value of either Le or Le_{eff} is not affected. However, the increase in Nu_C corresponds to a reduction in T at a given location as the volume of the sphere of influence is increased; this affects the transport properties and induces a reduction in Le . In contrast, no such monotonic behavior is observed for Le_{eff} due to the combined effect of the transport properties variation and the reduction in the gradients at larger Nu_C .

3.3. Isolated fluid drops: the C_7H_{16} - N_2 system

The validity of the above conclusions for other systems has been investigated by performing calculations for an application relevant to gas turbine engines and diesel engines: the C_7H_{16} - N_2 system. Examination of the molar enthalpies of the two compounds shows that of n -heptane to be smaller than that of nitrogen; since the molar mass of n -heptane is larger than that of nitrogen, Soret and

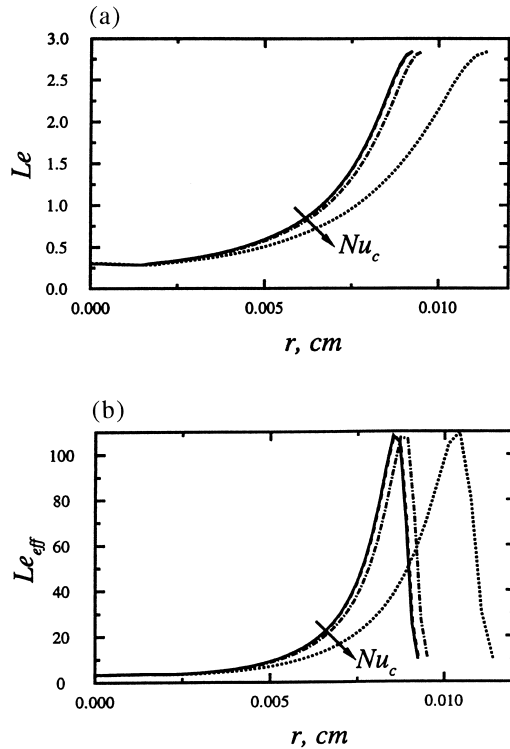


Fig. 7. Spatial variation at 10^{-2} s of the traditional (a) and the effective (b) Lewis numbers for $Nu_c = 10^2$ (—), 10^3 (---), 10^4 (---), and 10^5 (···). The other conditions are those of Fig. 6.

Dufour effects are again expected to be negligible. To ascertain this expectation, calculations were performed with $\alpha_T = 0.0, 0.01$ and 0.05 and it was found that the results were indeed virtually indistinguishable.

Figure 8 illustrates results from calculations for isolated heptane drops in nitrogen for the following conditions: $R_d^0 = 50 \times 10^{-4}$ cm, $R_{si}^0 = 0.03$ cm, $T_{d,b}^0 = 400$ K (T_d^0 is uniform inside the drop), $T_{si}^0 = T_e = 1000$ K, $p_e = 20$ MPa and $Y_{1e} = 0$. The ratio of Le_{eff} to Le is only approximately two for the maximum value independent of location, and approximately three locally. Similar to the LO_x - H_2 system, the variations of Le_{eff} and Le with r are different indicating again that Le is not a good qualitative measure of relative heat to mass transfer. Plots of Le_{eff} vs Le (not illustrated) paralleling those of Fig. 1(c) do not show the self-similar variation which seems to be a peculiarity of the LO_x - H_2 system.

4. Summary and conclusions

A model has been developed to calculate an effective Lewis number for situations where large gradients of species and temperature exist in a system. The model is

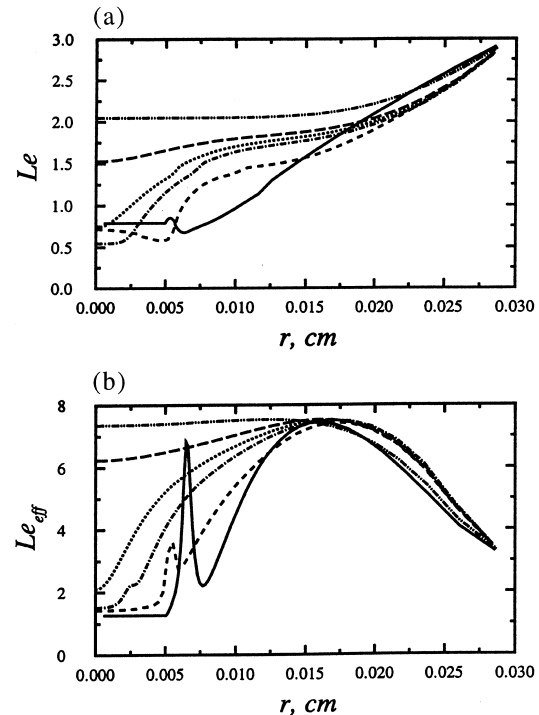


Fig. 8. Spatial variation of the traditional (a) and the effective (b) Lewis numbers for the n -heptane–nitrogen system for several times: 0.0 s (—), 10^{-2} s (---), 2×10^{-2} s (---), 2.25×10^{-2} s (···), 2.5×10^{-2} s (—), 3.3×10^{-2} s (---). Other initial conditions are: $R_d^0 = 50 \times 10^{-4}$ cm, $R_{si}^0 = 0.03$ cm, $T_{d,b}^0 = 400$ K, $T_{si}^0 = T_e = 1000$ K, $Y_{1e} = 0$ and $p = 20$ MPa.

based upon the assumption that derivatives of certain functions are small with respect to those of the dependent variables. Shvab–Zeldovich-like variables are defined to eliminate the coupling of the operators of the differential equations for species and energy. Based upon the new equations for the Shvab–Zeldovich-like variables, an effective diffusivity and thermal conductivity are defined and further calculated incorporating Soret and Dufour effects. The model is applied to binary component systems at supercritical conditions.

Results obtained for the isolated LO_x fluid drop in H_2 show that the effective Lewis number can be larger than the Lewis number by a factor of 40. Additionally, the traditional Lewis number and effective Lewis number have different spatial variations indicating that the traditional Lewis number is not even a qualitative measure of the relative importance of heat and mass transfer. Calculations performed by varying the value of the thermal diffusion factor indicate that it is not the Soret and Dufour terms that are responsible for the difference between the traditional and effective Lewis numbers. Instead, it is found that it is the combined effect of the small mass diffusion factor and transport effects of the

enthalpy with temperature gradients that are responsible for the enhancement in heat diffusion over mass diffusion. Similar calculations performed for fluid *n*-heptane drops in nitrogen showed the same trends in that the Soret and Dufour terms were unimportant within the range of values used for the thermal diffusion factors. For the *n*-heptane–nitrogen system, the effective Lewis number was only a factor of 2–3 larger than the traditional Lewis number. The uncertainty in the value and variation of the thermal diffusion factor with temperature, pressure and species molar fraction does not allow a definitive conclusion as to the importance of Soret and Dufour terms.

Parametric studies show that the effective Lewis number increases with increasing pressure and decreasing temperature, and that closer drop proximity results in sharper peaks in the effective Lewis number due to the increased gradients of the dependent variables.

Since the Lewis number is both a theoretically important quantity and a quantity used in simplified estimates by design engineers, the present findings have both a fundamental and a practical value.

Acknowledgements

This research was conducted at the Jet Propulsion Laboratory under sponsorship from the National Aeronautics and Space Administration, the George C. Marshall Space Flight Center with Mr Klaus W. Gross as technical contract monitor, and from the National Aeronautics and Space Administration, the Lewis Research Center with Drs Edward Mularz and Daniel L. Bulzan as technical contract monitors. Their continuing interest and support are greatly appreciated.

Appendix

The expressions for the elements of the flux matrix are as follows:

$$A_J = (m/m_1)nD_m\alpha_D \quad (\text{A.1})$$

$$B_J = (m_2/m)nD_m\{(m_1m_2X_1X_2/m)(h_2/m_2 - h_1/m_1)/(R_uT^2) + X_1X_2\alpha_T/T\} \quad (\text{A.2})$$

$$C_J = (m_2/m)nD_m(m_1m_2X_1X_2/m)(v_1/m_1 - v_2/m_2)/(R_uT) \quad (\text{A.3})$$

$$A_q = \lambda + (\alpha_T R_u T)nD_m(m_1m_2X_1X_2/m)(h_2/m_2 - h_1/m_1)/(R_uT^2) \quad (\text{A.4})$$

$$C_q = [m^2/(m_1m_2)]nD_m\alpha_D\alpha_T R_u T \quad (\text{A.5})$$

$$B_q = nD_m\alpha_T(m_1m_2X_1X_2/m)(v_1/m_1 - v_2/m_2). \quad (\text{A.6})$$

According to the Gibbs–Duhem relationship $\alpha_D = \alpha_{D1} = \alpha_{D2}$, where $\alpha_{D_i} = 1 + X_i(\partial \ln \gamma_i / \partial X_i)_{T,p}$.

References

- [1] C.K. Law, C.J. Sung, C.J. Sun, On the aerodynamics of flame surfaces, in: C.L. Tien (Ed.), Annual Review of Heat Transfer, vol. VIII, to appear.
- [2] D.C. Haworth, T.J. Poinot, Numerical simulations of Lewis number effects in turbulent premixed flames, *J. Fluid Mech.* 244 (1992) 405–436.
- [3] J.G. Lee, T.W. Lee, D.A. Nye, D.A. Santavicca, Lewis number effects on premixed flames interacting with turbulent Karman vortex streets, *Combust. Flame* 100 (1–2) (1995) 161–168.
- [4] G. Joulin, On the response of premixed flames to time-dependent stretch and curvature, *Combust. Sci. and Tech.* 97 (1–3) (1994) 219–229.
- [5] T. Echehki, J.H. Ferziger, Studies of curvature effects on laminar premixed flames—stationary cylindrical flames, *Combust. Sci. and Tech.* 90 (1–4) (1993) 231–252.
- [6] J.B. Greenberg, P.D. Ronney, Analysis of Lewis number effects in flame spread, *Int. J. Heat Mass Transfer* 36 (2) (1993) 315–323.
- [7] F.A. Williams, *Combustion Theory*, Addison-Wesley, 1965.
- [8] J. Keizer, *Statistical Thermodynamics of Nonequilibrium Processes*, Springer-Verlag, New York, 1987.
- [9] E. Peacock-Lopez, L. Woodhouse, Generalized transport theory and its application to binary mixtures, in: E. Matteoli, G.A. Mansoori (Eds.), *Fluctuation Theory of Mixtures*, Advances in Thermodynamics, vol. 2, Taylor and Francis, 1983, pp. 301–333.
- [10] K. Harstad, J. Bellan, Isolated fluid oxygen drop behavior in fluid hydrogen at rocket chamber pressures, *Int. J. Heat Mass Transfer* 41 (1998) 3537–3550.
- [11] Y. Tambour, B. Gal-Or, Phenomenological theory of thermodynamic coupling in multicomponent compressible laminar boundary layers, *Phys. Fluids* 19 (2) (1976) 219–226.
- [12] J.B. Greenberg, Y. Tambour, B. Gal-Or, A solution procedure for heat and mass transfer in multicomponent laminar jets, *Int. J. Heat Mass Transfer* 23 (1980) 1595–1598.
- [13] J.B. Greenberg, On the prediction of thermal diffusion effects in laminar one-dimensional flames, *Combust. Sci. Techn.* 24 (1980) 83–88.
- [14] K. Harstad, J. Bellan, Interactions of fluid oxygen drops in fluid hydrogen at rocket chamber pressures, *Int. J. Heat Mass Transfer* 41 (1998) 3551–3558.
- [15] J. Bellan, R. Cuffel, A theory of non-dilute spray evaporation based upon multiple drop interaction, *Combust. and Flame* 51 (1) (1983) 55–67.
- [16] R.B. Bird, W.E. Stewart, E.N. Lightfoot, *Transport Phenomena*, John Wiley and Sons, 1960.
- [17] K.G. Harstad, R.S. Miller, J. Bellan, Efficient high pressure state equations, *A.I.Ch.E. J.* 43 (6) (1997) 1605–1610.
- [18] E.L. Cussler, *Diffusion. Mass Transfer in Fluid Systems*, Cambridge University Press, 1984.